cut 1 μm thick, stained with methylene blue and azure II, and evaluated by light microscopy. To establish whether a neuroprotective effect was achieved, the tissue was evaluated by a rater who was blind to the experimental conditions. At least six retinal segments were examined for each experimental condition and these were matched with at least six concurrent controls. In the standard assay, an agonist was used at a fixed concentration (previously established in concentration-response studies as a threshold concentration that reproducibly causes a fully developed retinal lesion in 30 min: Glu, 1 m*M*; NMDA, 80 μ*M*; Quis, 15 μ*M*; or KA, 25 μ*M*), and excitatory amino acid antagonists were added to assess their ability to block the excitotoxic action of a given agonist. Although agents that are effective in antagonizing excitotoxic phenomena usually induce a partial blockade at concentrations lower than the threshold for total blockade, we used the concentration that totally prevented toxic activity for purposes of rating antagonist potency. To determine whether a given antagonist blocks an agonist toxic action by a competitive mechanism, we increased the concentration of agonist (for example, NMDA or L-Cys) in graduated steps and determined what concentration of antagonist was required to maintain a full blockade at each step.

7. J. C. Watkins and R. H. Evans, *Annu. Rev. Pharmacol. Toxicol.* **21**, 165 (1981).
8. J. W. Johnson and P. Ascher, *Nature* **325**, 529 (1987); J. A. Kemp *et al.*, *Proc. Natl. Acad. Sci. U.S.A.* **85**, 6547 (1988).
9. D. Lodge and N. A. Anis, *Eur. J. Pharmacol.* *77*, 203 (1982); J. A. Kemp, A. C. Foster, E. H. F. Wong, *Trends Neurosci.* **10**, 294 (1987).
10. T. Honoré *et al.*, *Science* **241**, 701 (1988); M. T. Price *et al.*, *Soc. Neurosci. Abstr.* **14**, 418 (1988).
11. M. Friedman, *The Chemistry and Biochemistry of the Sulfhydryl Group in Amino Acids, Peptides and Proteins* (Pergamon Press, New York, 1973), p. 27.
12. The ability of increasing concentrations of Zn^{2+} to block toxicity produced by increasing concentrations of L-Cys supports this interpretation since Zn^{2+} does not block toxicity mediated through Quis receptors. Therefore, the ability of Zn^{2+} to prevent increasing concentrations of L-Cys from inducing a Quis-type lesion implies that it formed complexes with L-Cys, thereby inactivating the L-Cys molecule.
13. J. W. Olney, M. T. Price, J. Labruyere, unpublished data. In the chick embryo retina, kynurenic acid is a broad spectrum antagonist that effectively blocks the toxic action of NMDA, Quis, or KA but is significantly more potent against NMDA (*6*). We have observed that 7-CK is approximately two times more potent than kynurenic acid in protecting retinal neurons against either NMDA, KA, or Quis neurotoxicity. Consistent with electrophysiological evidence (*8*) suggesting that 7-CK blocks NMDA responses by an action at the glycine site, we have found that the antagonism of NMDA neurotoxicity by 7-CK is reversible by adding glycine, and that 7-CK also blocks L-Cys neurotoxicity by a glycine-reversible mechanism.
14. J. H. Weiss and D. W. Choi, *Science* **241**, 973 (1988).
15. L. O. Trussell, L. L. Thio, C. F. Zorumski, G. D. Fischbach, *Proc. Natl. Acad. Sci. U.S.A.* **85**, 2834 (1988); C. E. Jahr and C. F. Stevens, *Nature* **325**, 522 (1987).
16. S. I. Rapoport, *Blood-Brain Barrier in Physiology and Medicine* (Raven Press, New York, 1976).
17. H. Benveniste, J. Drejer, A. Schousboe, N. M. Diemer, *J. Neurochem.* **43**, 1369 (1984).
18. J. W. McDonald, F. S. Silverstein, M. V. Johnston, *Brain Res.* **459**, 200 (1988); C. Ikonomidou *et al.*, *J. Neurosci.* **9**, 1693 (1989); C. Ikonomidou *et al.*, *ibid.*, p. 2809; J. W. Olney, C. Ikonomidou, J. L. Mosinger, G. Frierdich, *ibid.*, p. 1701.
19. P. S. Spencer *et al.*, *Science* **237**, 517 (1987).
20. M. T. Heafield *et al.*, *Neurosci Lett.* **110**, 216 (1990).
21. In the chick embryo retina, BMAA is not toxic in the absence of bicarbonate but becomes a weak toxin in the presence of physiologic concentrations of bicarbonate. The thresholds of BMAA and L-Cys for expressing excitotoxicity in the chick retina in the presence of physiologic concentrations of bicarbonate are approximately 3 m*M* and 300 μ*M*, respectively (G. R. Stewart, J. W. Olney, M. T. Price, unpublished data). Thus, L-Cys is ten times more potent than BMAA in this preparation.
22. Supported in part by HD 24237, DA 05072, and NIMH Research Scientist Award MH 38894 (J.W.O.), Physician Scientist Award MH 00630 (C.F.Z.) and Klingenstein Fellowship (C.F.Z.).

5 October 1989; accepted 8 March 1990

K^+ Current Diversity Is Produced by an Extended Gene Family Conserved in *Drosophila* and Mouse

AGUAN WEI, MANUEL COVARRUBIAS, ALICE BUTLER, KEITH BAKER, MICHAEL PAK, LAWRENCE SALKOFF

The *Drosophila Shaker* gene on the X chromosome has three sister genes, *Shal*, *Shab*, and *Shaw*, which map to the second and third chromosomes. This extended gene family encodes voltage-gated potassium channels with widely varying kinetics (rate of macroscopic current activation and inactivation) and voltage sensitivity of steady-state inactivation. The differences in the currents of the various gene products are greater than the differences produced by alternative splicing of the *Shaker* gene. In *Drosophila*, the transient (A current) subtype of the potassium channel (*Shaker* and *Shal*) and the delayed-rectifier subtype (*Shab* and *Shaw*) are encoded by homologous genes, and there is more than one gene for each subtype of channel. Homologs of *Shaker*, *Shal*, *Shab*, and *Shaw* are present in mammals; each *Drosophila* potassium-channel gene may be represented as a multigene subfamily in mammals.

POTASSIUM CHANNEL DIVERSITY IN *Drosophila* may result from an extended gene family coding for homologous proteins since the *Drosophila Shaker* gene (*1*) has three sister genes (*2*). The peptides encoded by the extended gene family *Shaker*, *Shal*, *Shab*, and *Shaw* share a conserved organization suggestive of common function (*2*). We now report that, like *Shaker*, the *Shal*, *Shab*, and *Shaw* gene products each expresses a K^+ current in the *Xenopus* oocyte system. Although the currents share general features (voltage-gating and K^+ selectivity), they differ greatly in their kinetic and voltage-sensitive properties.

Because of its resemblance to one of the four homologous domains of the Na^+ (*3*) and Ca^{2+} channels (*4*), the *Shaker* holoprotein is presumed to be a homotetramer (*5*). Like the peptide encoded by *Shaker*, the peptides encoded by *Shal*, *Shab*, and *Shaw* each form functional K^+ channels in *Xenopus* oocytes, all potentially function as homomultimers in vivo.

We have isolated cDNAs for two alternatively spliced mRNAs transcribed from *Shal* that encode the protein products Shal1 and Shal2 (*2*). The deduced amino acid sequence of Shal2 is compared to that of the conserved portions of *Shaker*, *Shab*, and *Shaw* cDNAs (Fig. 1A). Shal1 has a splice junction at residue 489 of Shal2 (Fig. 1A). In Shal1 the COOH-terminal residue from Shal2 (Met^{490}) is absent and 116 amino acids are added (*6*). The highly conserved regions of the deduced peptides include the hydrophobic domains, S1 through S6, which may be membrane-spanning structures (*1, 3*). One or more possible N-linked glycosylation sites, indicated by the consensus sequence Asn-X-Ser/Thr (*7*), are present between S1 and S2 in Shaker, Shab, and Shaw, but not in Shal. The deduced peptides for Shal2 of 490 amino acids (56 kD) and Shaw2 of 498 amino acids (56.5 kD) are somewhat smaller than Shaker, which average 71 kD. The deduced Shab peptide is the largest with 924 amino acids (100 kD). This size difference results from length variation in the domains at the NH_2- and COOH-termini, both of which are presumed to be cytoplasmic. The conserved core of Shaker, Shal, Shab, and Shaw encompassing the membrane-spanning portions S1 through S6 averages about 240 residues and varies little among the subfamily members. A pairwise comparison of homology for the entire conserved region (Shal residues 45 to 409) shows a degree of identity ranging from 38 to 42% among all four predicted peptide sequences (Fig. 1A).

Each member of the *Drosophila* gene family, *Shaker*, *Shal*, *Shab*, and *Shaw*, has one or more mammalian homologs, and thus, defines a subfamily for each member. A comparison of each fly K^+-channel protein to a homolog from mouse brain is shown in Fig. 1B. The mammalian homologs of the *Shaker* protein (*8*) are more closely related to the *Drosophila Shaker* protein (about 76% iden-

A. Wei, M. Covarrubias, A. Butler, K. Baker, M. Pak, Department of Anatomy and Neurobiology, Washington University School of Medicine, St. Louis, MO 63110.
L. Salkoff, Department of Anatomy and Neurobiology and Department of Genetics, Washington University School of Medicine, St. Louis, MO 63110.

tity through the conserved core) than to the other *Drosophila* K^+ channels coded by *Shal*, *Shab*, and *Shaw* (about 38% identity). A similar relation exists for the mammalian homologs of Shab (*9, 10*), Shaw (*10, 11*), and Shal (*10*); each has significantly higher homology to only one of the *Drosophila* proteins. The 36–amino acid region in Fig. 1B includes a domain where the proteins from all four subfamilies are identical (Shal residues 82 to 87) (Fig. 1A), but includes areas unique to each subfamily. Mouse and *Drosophila* Shal homologs have only 61% identity in the area shown in Fig. 1B, but other areas have higher interspecies homology; the Shal homologs are identical in a large area surrounding the S4 region (Shal residues 282 to 327) (Fig. 1A). It thus appears that the four subfamilies of K^+ channels evolved many of their individual structural features before the separation of vertebrate and invertebrate species.

For expression of the *Drosophila* K^+-channel genes in *Xenopus* oocytes, the ShakerH37 (*12*), Shal2, Shab11, and Shaw2 (*2*) cDNA clones were transcribed in vitro, and cRNA transcripts were injected into oocytes (*13*). Current records for each expressed gene product, Shaker, Shal, Shab, and Shaw, are shown in Fig. 2, A to D. In each case the membrane was held at −90 mV, and depolarizing voltage-clamp step pulses were applied in 10-mV increments until a value of +20 mV was reached. The data for Shaker and Shal were recorded at 11°C so as to resolve the peaks of these more rapid currents (Fig. 2, A and B). Shab and Shaw currents were recorded at room temperature to show the slow rates of activation and current decay (Fig. 2, C and D).

To compare relative rates of current activation, we measured the rise time to 95% of maximum current for voltage-step pulses to 0 mV from a holding potential of −90 mV (Table 1). Shaker and Shal have fast rise times (11 ms and 25 ms, respectively, at 23°C) relative to Shab (176 ms) and Shaw

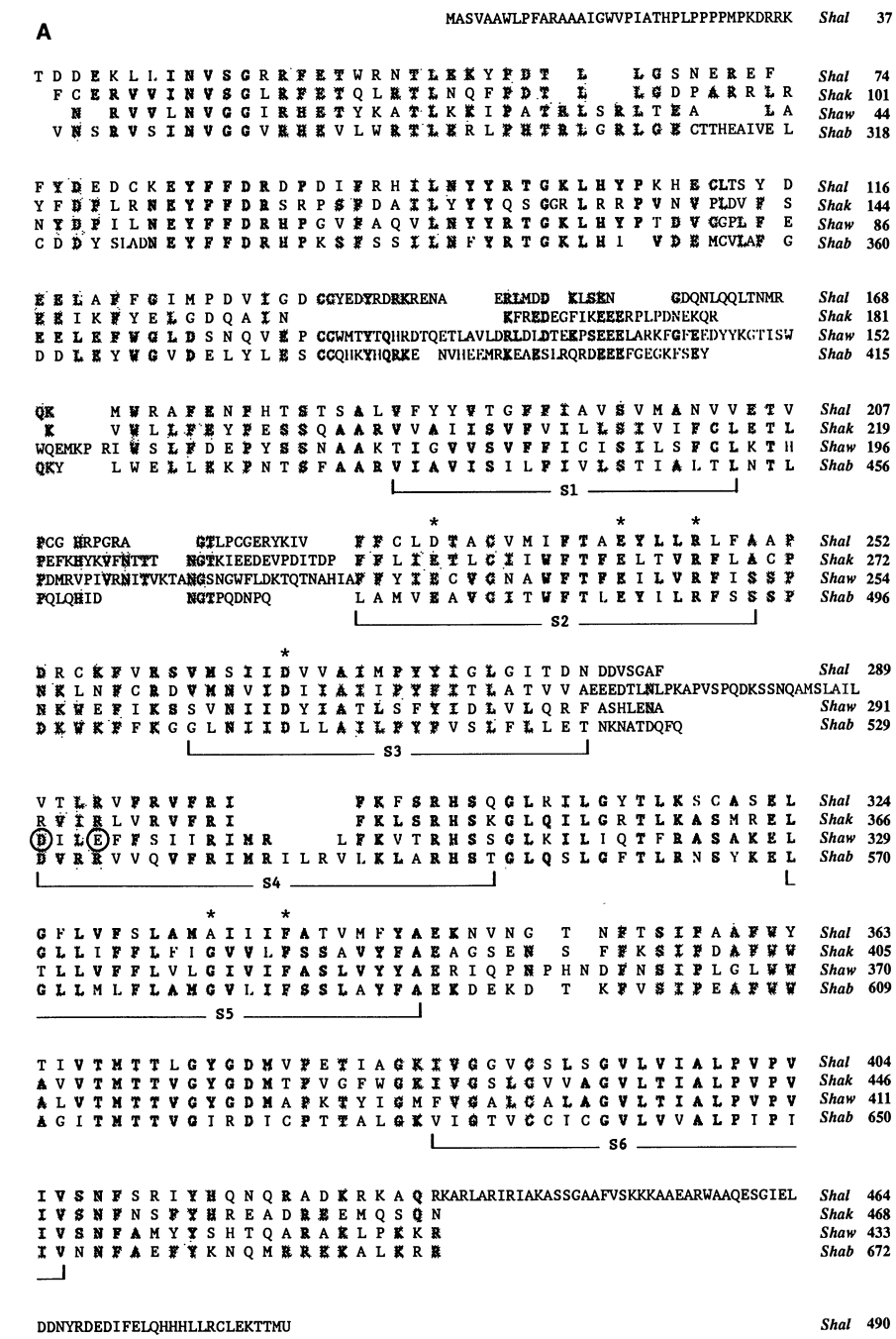

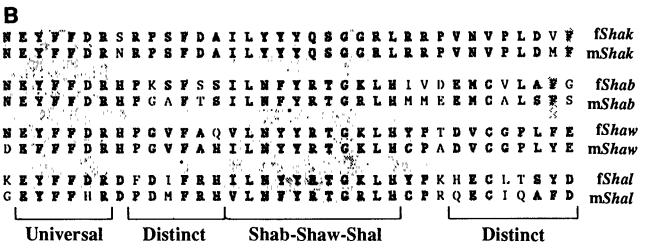

Fig. 1. (**A**) Sequence of the *Drosophila* extended gene family of K^+-channel cDNAs. The deduced amino acid sequence for Shal2 is compared to that of the conserved portions of ShakerH37 (*11*), Shaw2 (*2*), and Shab11 (*2*). Two or more identical residues in the same corresponding position are shaded. Proposed membrane-spanning regions are underlined and designated S1 to S6. Asterisks indicate conserved residues present in most voltage-gated channels including the Na^+ (*3*) and Ca^{2+} (*4*) channels. The single letter amino acid code is A, Ala; C, Cys; D, Asp; E, Glu; F, Phe; G, Gly; H, His; I, Ile; K, Lys; L, Leu; M, Met; N, Asn; P, Pro; Q, Gln; R, Arg; S, Ser; T, Thr; V, Val; W, Trp; Y, Tyr; and U, Stop. Sequencing of both strands of the *Shal2* cDNA was achieved with M13 single-strand cloning vectors mp18 and mp19. A series of overlapping deletions in single-stranded DNA were constructed with the single-strand exonuclease activity of T4 polymerase (IBI Cyclone Kit). Synthetic primers were also used. (**B**) K^+-channel subfamilies are conserved between *Drosophila* (fShak, fShab, fShaw, and fShal) and mouse brain (mShak, mShab, mShaw, and mShal); mShak is MBK1 from Tempel *et al.* (*8*). The 36-residue area shown begins with Shal residue 81 (A). Residues present with two or more peptides are shaded; similar groups of residues in different subfamily peptides are bridged by shading. The alignment in this figure is without gaps to show interspecies length conservation in each subfamily. Conserved groups of residues are present within this region that are common to all four subfamilies (universal), unique to each subfamily (distinct), or common to Shab, Shaw, and Shal, but absent in Shaker (Shab-Shaw-Shal). The percent identity in this region for interspecies subfamily homologs is Shaker, 94%; Shab, 72%; Shaw, 83%; and Shal, 61%.

(102 ms).

The Shaker current has a rapid time-dependent current decay that was fitted by a single exponential with a time constant of 238 ms at +20 mV (11°C). The Shal current decay was slower and was better fitted by the sum of two exponentials, the faster component having a time constant of 480 ms. Shab and some Shaw currents decayed very slowly with time constants of several seconds. For Shaker and Shal, the rate of current decay varied little among different injected oocytes. For Shab and Shaw, however, the rate of current decay was variable, but always much slower than that of Shal. However, whereas all Shab currents showed an obvious current decay during a long (10-s) pulse, most Shaw currents showed none.

We measured the current-voltage relations for these channels (Fig. 2, E to H). Shaker, Shal, and Shab currents have a steep current-voltage relation, and all three appear to activate sharply between −50 and −40 mV. In contrast, in all of the oocytes showing Shaw expression (Table 1), the current activated more gradually beginning at −70 mV. Thus, the voltage sensitivity (*14, 15*) of Shaw seems distinct from the other three channels.

All voltage-gated channels that belong to the supergene family, including Na^+ and Ca^{2+} channels and the *Shaker* extended family of K^+ channels, have a string of positive charges in the S4 region that may be the voltage sensor of the channel. The positive charges are in the configuration +00, where + signifies a positively charged residue and 0 signifies a neutral residue. Site-directed mutations that alter these charges in the Na^+ channel affect gating in a manner suggesting that these charges are, indeed, the voltage sensor (*16*). Whereas the Shaker protein has seven charges in the string, the Shaw protein has only four positive charges in an uninterrupted +00 string. In addition, two of the omitted charges have been replaced with negative charges; aspartic acid and glutamic acid (Fig. 1A, circled Shaw residues 292 and 295 in the S4 region) are at positions where these charges might sense the transmembrane electric field.

The voltage sensitivity of steady-state inactivation is one of the parameters that define the voltage range in which a channel may be active (*14, 15*). This property is invariant among all alternative Shaker forms (*12*). However, it differs substantially among Shal, Shab, and Shaw. Shal channels have the most hyperpolarized steady-state inactivation curve with a midpoint at −62 mV (Fig. 3A), and thus more closely resemble the transient K^+ channels characterized in neurons of other systems (*17*). In addition, the slope of the steady-state inactivation curve for Shal is shallow relative to that of the other currents (Table 1). The steady-state inactivation curves for Shab (midpoint, −50 mV) (Fig. 3A) and Shaker (midpoint, −49 mV) (Fig. 3A) are comparable, although Shaker has a steeper slope than the other channels. The typical Shaw current displays no steady-state inactivation.

As expected for K^+-selective channels, Shaker, Shal, and Shab currents have reversal potentials close to the calculated K^+ equilibrium potential (−80 mV in 2 m*M* extracellular K^+). In contrast, the Shaw reversal potential is more depolarized, approximately −60 mV. In ion substitution experiments, the three channels, Shaker, Shal, and Shab, seem to have comparable K^+ selectivity as indicated by the similar slopes of the curves in Fig. 3B, whereas the more shallow slope for Shaw indicates less K^+ selectivity.

The Shaker current is inhibited by 4-aminopyridine (4-AP) (*12*). Shal peak current was inhibited 31 ± 9% (mean ± SD; $n = 3$) by 1 to 2 m*M* 4-AP and 2 ± 4% ($n = 4$) by 10 m*M* tetraethylammonium chloride (TEA). The Shab current, on the other hand, was less inhibited by 4-AP (6 ± 4%; $n = 3$), but more by TEA (50 ± 5%; $n = 3$), consistent with the pharmacology of other delayed rectifier subtypes of K^+ channels (*13*). In contrast to Shab, the Shaw current, which also resembles a delayed rectifier in its activation and decay properties, has the reverse sensitivities; it is more inhibited by 4-AP (80 ± 6%, $n = 3$) than TEA (8 ± 1%, $n = 2$).

The finding that the Shal, Shab, or Shaw products alone, like the Shaker product, can form voltage-gated K^+ channels suggests that voltage-gated K^+ channels can function as homomultimers. Thus, gene duplication may be a major mechanism of generating diversity for K^+ channels, as it appears to be for other important proteins. Shal plus Shab and Shal plus Shaw do not seem to form hybrid channels when coexpressed in *Xenopus* oocytes, suggesting that they are independent channel systems (*10*).

Several of the mammalian homologs of

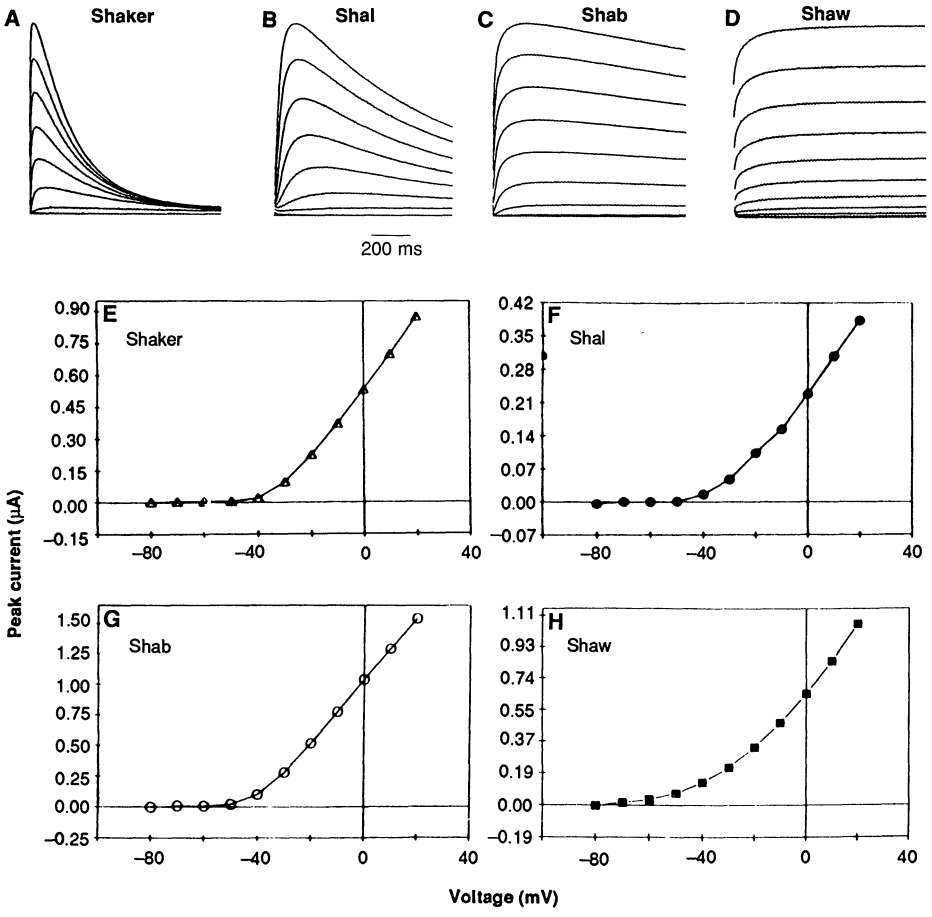

Fig. 2. Expression of K^+ currents in *Xenopus* oocytes injected with ShakerH37 (*Shaker*), Shal2 (*Shal*), Shab11 (*Shab*), and Shaw2 (*Shaw*) cRNAs. (**A** to **D**) Outward currents recorded in response to 1-s voltage-step depolarizations ranging between −80 and +20 mV in 10-mV steps from a holding potential of −90 mV. For clarity, the capacitative currents were deleted. Records were leak subtracted assuming a linear leak current. (**E** to **H**) The corresponding peak current-voltage relations are shown for (E) Shaker (△), (F) Shal (●), (G) Shab (○), and (H) Shaw (■). The Shaker, Shal, and Shab currents turn on abruptly at about −50 mV, whereas the *Shaw* current has a more gradual response to voltage.

Table 1. Electrophysiological parameters of Shaker, Shal, Shab, and Shaw K^+ channels expressed in oocytes. Peak currents are given as median values and range. Rise times are given for the current evoked by a voltage-clamp step pulse to 0 mV from a holding potential of −90 mV. Shal inactivation curves were best fit by the sum of two expotentials. Only the fast component is shown. The fastest inactivation observed had time constants greater than several seconds. The number of experiments is shown in parentheses; error limits are ±SD.

Gene	Peak current at 20 mV (nA) median range	Activation threshold (mV)	Rise time (ms) to 95% of maximum current	τ of inactivation at 20 mV* (ms)	Steady-state inactivation $V_{1/2}$ (mV)	Slope factor (mV/*e*-fold)	K^+ selectivity†
ShakerH37	706 (8) 501–1357	−50 to −40 (9)	31 ± 7 (8)* 11 (1)	238 ± 63 (8)	−49 ± 2 (7)	3.5 ± 0.3 (7)	50 (1)
Shal	666 (12) 233–1078	−50 to −40 (15)	124 ± 25 (5) * 26 ± 4 (11)	480 ± 180 (4)	−62 ± 1 (4)	7.3 ± 0.9 (4)	47 (2)
Shab	850 (7) 340–1540	−50 to −40 (7)	176 ± 77 (9)	Very slow	−50 ± 3 (4)	6.8 ± 0.9 (4)	53 (2)
Shaw	702 (19) 231–1170	−80 to −70 (19)	102 ± 30 (7)	None	None		33 (4)

*11°C; other experiments are at 23C°. †Refers to change in reversal potential in millivolts for a tenfold change in extracellular K^+ concentration.

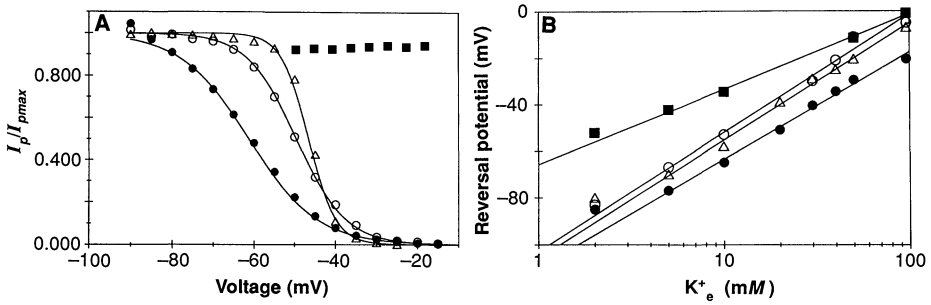

Fig. 3. Comparison of (**A**) steady-state inactivation and (**B**) reversal potentials for channels coded by *Shaker* (△), *Shal* (●), *Shab* (○), and *Shaw* (■). Steady-state inactivation of Shaker, Shal, and Shab was fit by a single Boltzmann equation. Peak currents were measured by a test pulse to +20 mV after a 10-s prepulse. Prepulses were applied from −90 to −10 mV in increments of 5 mV. In the 20-s interval between voltage pulses the membrane was returned to −90 mV. The Shaker current had to be held at −120 mV for part of this interval to fully recover from inactivation. The solid lines are the best fits to a single Boltzmann function: $I_p/I_{pmax} = 1/(1 + \exp(V_m - V_{1/2})/a)$, where I_{pmax} is the maximum peak current, I_p is the peak current at a given V_m, a is the slope factor, and $V_{1/2}$ is the voltage at which half of the channels become inactivated. The Shal current is the most hyperpolarized (~60 mV), whereas Shab and Shaker currents are intermediate (−45 to −50 mV). The Shaker current has the steepest voltage dependence. The Shaw current showed no inactivation in these experiments. The data points for Shaw more negative than −50 mV have been omitted to avoid obscuring the data points for the other currents. (**B**) The reversal potentials of tail currents. The curves for Shaker, Shal, and Shab currents approximate the theoretical Nernst relationship as expected for a channel selectively permeable to K^+ ions. The more shallow curve for the Shaw current suggests less selectivity (slopes estimated by linear least-square regression analysis of the data): Shaker, 50 mV per tenfold change in extracellular K^+ concentration; Shal, 47 mV; Shab, 53 mV; and Shaw, 33 mV. When the extracellular K^+ concentration was changed, the concentration of Na^+ ion was correspondingly changed, so that the extracellular concentration of monovalent cations was constant.

the *Drosophila* K^+-channel subfamilies have been expressed (*8–11*). The channels coded by the mammalian and *Drosophila Shaker* genes are similar in having rapid current activation. However, the mammalian currents have a much slower rate of current inactivation than the *Drosophila* current. In this aspect they resemble the delayed rectifier type of K^+ channel, rather than the transient A current type (*17*). Even RCK4, the fastest inactivating mammalian *Shaker* homolog (*8*), inactivates at a slower rate than the *Drosophila Shaker* A current (*1*). The mammalian brain and *Drosophila* Shab currents are similar in having both a slow rate of current rise and a slow rate of current decay (*9, 10*). The mammalian Shaw current also resembles a delayed rectifier type of K^+ channel (*11*). Thus, a rapidly inactivating A current (*17*) has not been observed from expression of a mammalian clone from brain. The mouse brain Shal homolog (*10*) has not yet been expressed.

Extensive alternative splicing of the primary gene transcript, like that observed at the *Shaker* locus in *Drosophila*, has not been observed in mammals for any K^+ channel. Instead, gene duplication has occurred within the mammalian *Shaker* subfamily, possibly as an alternative mechanism for producing variation. There are at least five *Shaker* subfamily genes (*8*) and three *Shaw* subfamily genes (*10, 11*). It is possible that gene duplication within a K^+-channel subfamily has been a recent event in vertebrate evolution and, thus, different numbers of *Shaker*, *Shal*, *Shab*, and *Shaw* subfamily genes may be found in different species.

REFERENCES AND NOTES

1. D. M. Papazian *et al.*, *Science* **237**, 749 (1987); A. Kamb *et al.*, *Neuron* **1**, 421 (1988); O. Pongs *et al.*, *EMBO J.* **7**, 1087 (1988); T. L. Schwartz *et al.*, *Nature* **331**, 137 (1988); L. C. Timpe *et al.*, *ibid.*, p. 143.
2. A. Butler, A. Wei, K. Baker, L. Salkoff, *Science* **243**, 943 (1989).
3. M. Noda *et al.*, *Nature* **312**, 121 (1984).
4. T. Tanabe *et al.*, *ibid.* **328**, 313 (1987).
5. C. Stevens, *ibid.*, p. 198; W. S. Agnew, *ibid.* **331**, 114 (1988).
6. Nucleotide sequences are filed with GenBank under the following accession numbers: *Shal*, M32660; *Shab*, M32659; and *Shaw*, M32661. A. Butler, A. Wei, L. Salkoff, *Nucleic Acids Res.*, in press.
7. R. Kornfeld and S. Kornfeld, *Annu. Rev. Biochem.* **54**, 631 (1985).
8. A. Baumann, A. Grupe, A. Ackermann, O. Pongs, *EMBO J.* **7**, 2457 (1988); B. L. Tempel, Y. N. Jan, L. Y. Jan, *Nature* **332**, 837 (1988); M. J. Christie, J. P. Adelman, J. Douglass, R. A. North, *Science* **244**, 221 (1989); D. McKinnon, *J. Biol. Chem.* **264**, 8230 (1989); W. Stuhmer *et al.*, *EMBO J.* **8**, 3235 (1989); K. G. Chandy *et al.*, *Science* **247**, 973 (1990).
9. G. Frech *et al.*, *Nature* **340**, 642 (1989).
10. M. Pak *et al.*, unpublished observations.
11. S. Yokoyama *et al.*, *FEBS Lett.* **259**, 37 (1989).
12. L. E. Iverson *et al.*, *Proc. Natl. Acad. Sci. U.S.A.* **85**, 5723 (1988).
13. *Shal*, *Shab*, *Shaw*, and *Shaker* cDNAs were subcloned into the polylinker of a plasmid transcription vector (Bluescript II, Stratagene). Capped run-off transcription reactions were performed with 1 to 5 μg of linearized template DNA, 1 m*M* nucleotide triphosphates, 1 m*M* G(5′)ppp(5′)G (cap analog), and 20 units of T7 or T3 RNA polymerase, in standard transcription buffer at 37°C for 1 hour. Transcription reactions were checked by sizing on 1.5% agarose gels. Before injection with cRNA, *Xenopus laevis* oocytes (stages 4 to 6) were incubated for 2 hours in collagenase (10 mg/ml) (type IA, Sigma) in ND96 without Ca^{2+} (96 m*M* NaCl, 2 m*M* KCl, 1 m*M* $MgCl_2$, and 5 m*M* Hepes, *p*H 7.5). Oocytes were pressure-injected with ~50 nl (approximately 100 ng) of cRNA in water and incubated in ND96 (as above, plus 1.8 m*M* $CaCl_2$), supplemented with 2.5 m*M* sodium pyruvate, penicillin (100 units/ml), and streptomycin (100 μg/ml), at 19°C for 2 to 4 days. A conventional two-microelectrode voltage clamp was used to record macroscopic currents in ND96. DIDS (4,4′-diisothiocyanatostilbene-2,2′-disulfonic acid) (1 m*M*) was added to block the endogenous Ca^{2+}-dependent Cl^- current (*17*). Cur-

rent records were filtered at 1 kHz with an 8-pole Bessel filter and acquired digitally with CCURRENT and analyzed by CQUANT (software written by K.B.). Recordings were performed at room temperature (22° to 23°C) or at 11°C, with a Peltier plate (Cambion).
14. B. Hille, *Ionic Channels of Excitable Membranes* (Sinauer, Sunderland, MA, 1984).
15. A. L. Hodgkin and A. F. Huxley, *J. Physiol. (London)* **116**, 449 (1952).
16. W. Stuhmer *et al.*, *Nature* **339**, 597 (1989).
17. J. A. Connor and C. F. J. Stevens, *J. Physiol. (London)* **213**, 21 (1971); B. Rudy, J. Hogar, H. Lester, N. Davidson, *Neuron* **1**, 649 (1988).
18. We thank A. Ratcliff for technical assistance and P. De Weer, J. Krause, J. H. Steinbach, E. McClesky, and G. Fischbach for their helpful comments. The *ShakerH37* Bluescript plasmid was provided by M. Tanouye. The *Drosophila* cDNA library was provided by P. Salvaterra. Supported by NIH grant 1 RO1 NS24785-01, a research grant from the Muscular Dystrophy Association of America, and a research grant from Searle, Inc. K.B. is partially supported by NIHRSA grant GMO 7200.

13 November 1989; accepted 26 February 1990

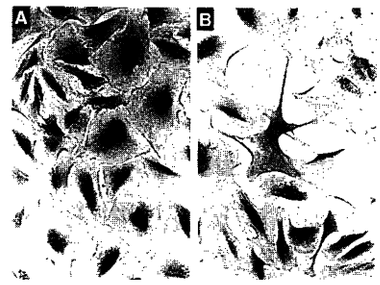

Fig. 1. (**A** and **B**) Morphology of undifferentiated HCN-1A cells (*10*), which appear polygonal with only occasional short processes (B). Magnification ×400.

Human Cortical Neuronal Cell Line: Establishment from a Patient with Unilateral Megalencephaly

GABRIELE V. RONNETT, LYNDA D. HESTER, JEFFREY S. NYE, KAREN CONNORS, SOLOMON H. SNYDER*

A cell line has been established in continuous culture of human cerebral cortical neurons obtained from a patient with unilateral megalencephaly, a disorder associated with continued proliferation of immature neuronal cells. When differentiated in the presence of nerve growth factor, 1-isobutyl-3-methylxanthine, and dibutyryl adenosine 3′,5′-monophosphate (cAMP), the cells display mature neuronal morphology with numerous long, extensively branched processes with spines and varicosities. The cells stain positively for neurofilament protein and neuron-specific enolase (selective neuronal markers) but are negative for glial markers, such as glial fibrillary acidic protein, S-100, and myelin basic protein. The cells also stain positively for the neurotransmitters γ-aminobutyric acid (GABA), glutamate, somatostatin, cholecystokinin-8, and vasoactive intestinal polypeptide. These cells may facilitate characterization of neurons in the human central nervous system.

THE GREAT HETEROGENEITY OF THE central nervous system (CNS) has precluded extensive molecular characterization of individual types of CNS neurons, which might be overcome through the use of continuous cultures. Techniques previously utilized to establish cell lines can have limitations. Primary cultures are heterogeneous and have limited life-spans, whereas cell lines derived from malignant tumors and somatic cell hybrids may differ from the mature neuronal phenotype. Here we have utilized cerebral cortical tissue from a patient with unilateral megalencephaly, a low-grade proliferation and migration disorder of neurons, to establish a human cortical neuronal cell line.

We obtained cerebral cortical tissue from an 18-month-old female undergoing hemispherectomy for intractable seizures (*1*). Dissociated cells from gray matter were immediately plated in medium containing serum. After 21 days all cells had died except for two small foci of growth, which were cloned and designated HCN-1 and HCN-4. These cells have been passaged more than 20 times in the course of 19 months with no significant changes in morphology or growth characteristics (*2*).

Although both of these cell lines originated from small foci of growth in culture, to ensure clonality we subcloned them; one of these attempts yielded a subclone from HCN-1 cells, designated HCN-1A. Both the parental and subcloned line have identical growth and staining characteristics, and therefore all further comments are restricted to the HCN-1A cell line. HCN-1A cells appeared epithelioid (Fig. 1, A and B) and rarely extended short processes (Fig. 1B). Cells grew to confluence but were contact-inhibited beyond this density. Doubling time was approximately 72 hours. Karyotype analysis demonstrated a chromosomal number of 46 ± 2 (*3*).

We examined the influence of various agents on the growth and morphology of HCN-1A cells. Nerve growth factor (NGF), insulin, dexamethasone, the phorbol ester 12-*O*-tetradecanoyl phorbol-13-acetate (TPA), ascorbic acid, dibutyryl cAMP, 1-isobutyl-3-methyl xanthine (IBMX), and retinoic acid were examined alone and in various combinations. The most mature morphology, with considerably slowed growth (a doubling time of 120 hours), occurred in cells grown with a mixture of IBMX, NGF, and dibutyryl cAMP (*4*). The undifferentiated HCN-1A cells were generally flat and polygonal with occasional short, unbranched processes. By contrast, the differentiated cells displayed round cell bodies with numerous, long and extensively branched processes with spines and varicosities. The differentiated cells were either bipolar or multipolar (Fig. 2). One hundred percent of cells differentiated over a 3-day period. Withdrawal of the differentiating agents caused retraction of processes, but cellular division remained slow with a doubling time of more than 120 hours.

To further characterize the cells, we stained them with antibodies to neurofila-

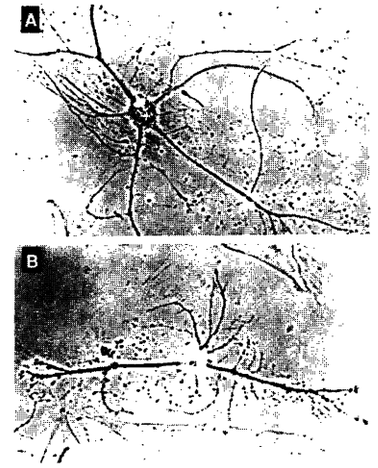

Fig. 2. Morphology of differentiated HCN-1A cells (*4*). Whereas undifferentiated cells were flat and polygonal, differentiated cells demonstrated multipolar (**A**) or bipolar (**B**) morphologies. All cells had spines and varicosities along their processes.

G. V. Ronnett, Department of Neurology and Department of Neuroscience, Pharmacology, and Molecular Sciences, Johns Hopkins University School of Medicine, Baltimore, MD 21205.
L. D. Hester and J. S. Nye, Department of Neuroscience, Johns Hopkins University School of Medicine, Baltimore, MD 21205.
K. Connors, Department of Physiology, Johns Hopkins University School of Medicine, Baltimore, MD 21205.
S. H. Snyder, Department of Neuroscience, Pharmacology, and Molecular Sciences and Department of Psychiatry and Behavioral Sciences, Johns Hopkins University School of Medicine, Baltimore, MD 21205.

*To whom correspondence should be addressed.